Dispersant Effects on Waterborne Oil Profiles and Behavior during the Deepwater Horizon Oil Spill

James R. Payne, Ph.D.   **August 2015**

William B. Driskell

Dispersants were liberally applied to *Deepwater Horizon* (DWH) surface slicks but also, unique to this spill, they were injected at the wellhead. The primary objective of dispersant remediation at depth was to enhance breakup of oil into smaller micro-droplets, which subsequently rise slower through the water column and weather quicker. Subsurface application of dispersants was also believed to reduce response personnel exposure to volatile aromatic and aliphatic components after larger oil droplets eventually reached the surface (Ryerson et al., 2011). When applied to surface slicks, dispersed oil weathers quicker and remains entrained in near-surface waters where it is less susceptible to being wind-driven into intertidal habitats (NRC 2005; Katz 2009). Approximately 1,070,000 gallons were applied to the surface from aircraft and boats, ~80% as the Corexit 9500 formulation and ~20% as Corexit 9527, while an additional 771,000 gallons of Corexit 9500 were injected subsurface into the oil plume directly at the wellhead (Stout 2015a).

While evaluating more than 9,200 offshore and nearshore water samples (Payne and Driskell 2015a, 2015b, Driskell and Payne 2015), the presence of dispersant was indicated by detection of the active surfactant component, dioctyl-sulfosuccinate sodium salt (DOSS) or other dispersant indicators. DOSS was analyzed in water samples by ALS laboratory in Kelso, WA (previously CAS) and various academic labs using a newly developed high-performance liquid chromatography/mass spectrometry (LC/MS) method (Gray et al., 2011 and Kujawinski, et al. 2011). However, at Alpha Laboratory, standard gas chromatography/selected-ion-monitoring mass spectroscopy (GC/MS) was used to semi-quantify Corexit-derived components in water samples not requiring fractionation or cleanup (Stout 2015a). Dispersant indicators reported by Alpha included:

- 2-butoxyethanol, abbreviated herein as "2BE", a major solvent in Corexit 9527 but also a contaminant in filters used to field-extract samples' particulate-phase oil,
- di(propyleneglycol)-n-butyl ethers, abbreviated as "GE" for glycol ethers (and in some literature abbreviated DPnB), one of the major solvents in Corexit 9500 and
- bis(2-ethylhexyl)fumerate, a DOSS-derived, GC injection port heat-breakdown product associated with both Corexit 9527 and 9500 (Stout 2015a).

Concentrations presented herein are reported in ng/L (ppt) for both dissolved-phase and particulate-oil (filter) samples. Unique hydrocarbon distributions were noted as a dispersant effect and taken to confirm the effectiveness of deepwater dispersant application. Of the 9,200 forensically categorized water samples, 321 were forensic matches to DWH oil (MC252) also having dispersant-mediated profiles.

Dispersant Effects

As noted above, the primary objective of dispersants is to break up oil—a task accomplished by attaching the surfactant's oleophilic molecular end to oil's surface in sufficient concentration to reduce the oil's

1

surface tension and thereby create a micro-eruption of the oil droplet that reforms into smaller micro-droplets (Katz 2009, Gopalan and Katz 2010, Aprin et al. 2015). Gopalan and Katz demonstrated that at the sub-millimeter scale, a crude oil droplet mixed with dispersant shears into formations of localized regions with low surface tension that produce very long, micron-sized oil threads trailing behind the droplets (Figure 1 and Figure 2). Eventual breakup of these threads into micron-sized droplets presumably occurs due to reduction of surfactant concentration, as the surface area increases and the water-soluble dispersant diffuses into the surrounding fluid. The shearing may be caused by interaction with micro-scale turbulence from a simple buoyant rise or from mega-scale sources such as splashing rainfall or breaking waves (Figure 2, Murphy et al. 2015). Aprin et al. (2015) also note that with dispersant, the reduced surface tension allows spherical oil droplets to transform into the ellipsoid, filament and "cap" forms, which also increases their frictional drag, inducing turbulence and slowing their buoyant ascent. They also suggest that reduced surface tension should inhibit droplets from re-coalescing.
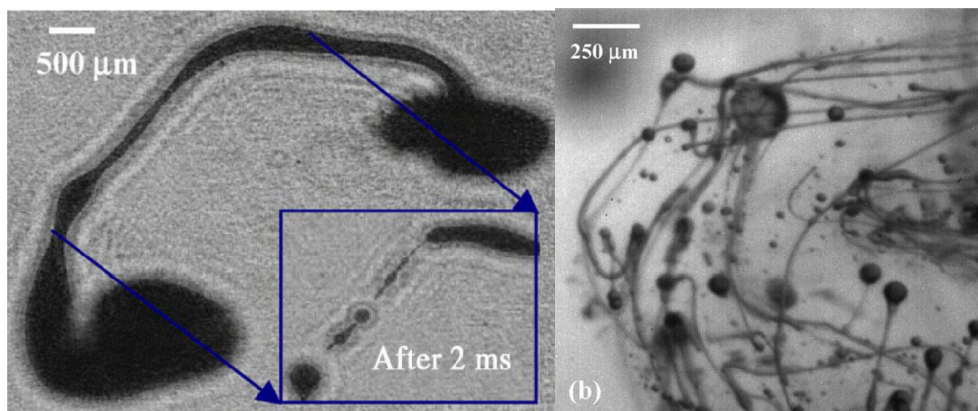

Figure 1. Images showing a) turbulent stretching of a crude oil droplet for disperant-to-oil ratio (DOR) of 1:20, with inset showing the capillary breakup of a section 2 ms later, and b) droplets with long threads trailing behind them, which are produced when a water jet impinges on a surface layer of oil mixed with dispersant (DOR 1:15)). (Images used with permission from Balaji, Gopalan and Joseph Katz, Johns Hopkins University).

Figure 2. Dispersed oil droplet shedding microdroplets while rising. (Image used with permission from David Murphy and Cheng Li, Johns Hopkins University)

The DWH-applied Corexit dispersants were lab and field-tested (under DWH response SMART monitoring protocols, Bejarano et al 2013) to empirically demonstrate their effectiveness. However, one effect that was assumed but not previously proven was that dispersant-treated oil droplets, because of their smaller droplet size and resulting very high surface-area-to-volume ratio, could lose their water-soluble, lower-molecular-weight polycyclic aromatic hydrocarbons (PAH) more quickly than non-dispersed oil (NRC 2005), i.e., they would weather quicker–an obviously important factor in evaluating dispersed-oil's dissolved-phase bioavailability/toxicity and modeling both non-dispersed and dispersant-treated oil's fate and behavior. Payne and Beegle-Krause (2011) demonstrated the correlation of subsurface dispersant components and the dissolved/particulate-phase oil in the water column but could not determine if the subsurface injection of the dispersants actually enhanced the breakup of the oil into smaller droplet sizes.

Also, prior to the DWH oil spill, it had not been documented that DOSS and the glycol ethers indicators would be conserved (Gray et al., 2011, 2014; White et al., 2014). Kujawinski, *et al.* (2011) found evidence of DWH dispersants within the depth range and fluorescent indications of the deep plume persisted up to 300 km from the well and 64 days after deepwater dispersant applications ceased but they didn't analyze those samples for PAH. Our forensic reviews found dispersant indicators at plume depth with dissolved oxygen (DO) and fluorescent confirmations, 412 km from the wellhead (Payne and Driskell, 2015a).

Dispersant-mediated Samples

During forensic analyses of the Natural Resource Damage Assessment (NRDA) water samples, dispersant-derived components were, for the first time, positively identified in field samples as truly attached to the oil droplets, viz., appearing in the filtered, oil-phase samples (particulate droplets only) and not in the dissolved-phase filtrate (methods in Payne and Driskell 2015b, 2015c). Furthermore, the dispersant-mediated samples presented unusual weathering patterns with a unique, accelerated, abiotic dissolution of the lower- and intermediate-molecular-weight PAH (through C3-dibenzothiophene, DBT3, Figure 3). Normal dissolution correlates with degree of alkylation within each PAH group in a fairly linear manner, i.e., when plotting histograms of individual PAHs arranged in order from lowest to highest molecular weights, dissolution results in preferential losses of parent and less alkylated compounds, such that the oil's unweathered "hump" distribution pattern is changed into a staircase pattern (Fig. 3). The term, "accelerated" dissolution, refers to the selective loss of the PAH in excess of a "normal" water-washed pattern at such an early stage of weathering. Dispersants accelerate the loss of the lower alkylated PAH.

This effect is seen in a comparison of dispersant-mediated versus non-dispersed field samples (Figure 4). Normalizing all values to each sample's conservative C2-chrysene effectively adjusts the values for weathering. Plotting the normalized values as bivariate scatterplots demonstrates the weathering patterns for the two analytes and their dispersant treatment (groups). No attempt was made to adjust for the amount of dispersant present relative to total PAH (TPAH). In reviewing the plots, the treatment groups for the various alkylated naphthobenzothiophene (NBT) isomers (bottom row) tend to appear in overlapping patterns, suggesting, as expected for these conservative analytes, very little weathering occurred. In contrast, the C2- versus C3-phenanthrenes' shift in group patterns (middle second row) implies these dispersed samples were weathering much faster than the non-dispersed samples. Similar effects are seen in all comparisons whereby statistically, 9 of the 14 showed significant differences in bivariate location of the two groups (Table 1) (using a nonparametric Mann-Whitney U test per Tabesh et

al., 2010). As mentioned above, this accelerated weathering is likely an enhanced dissolution effect as dispersants successively create smaller and smaller oil droplets.
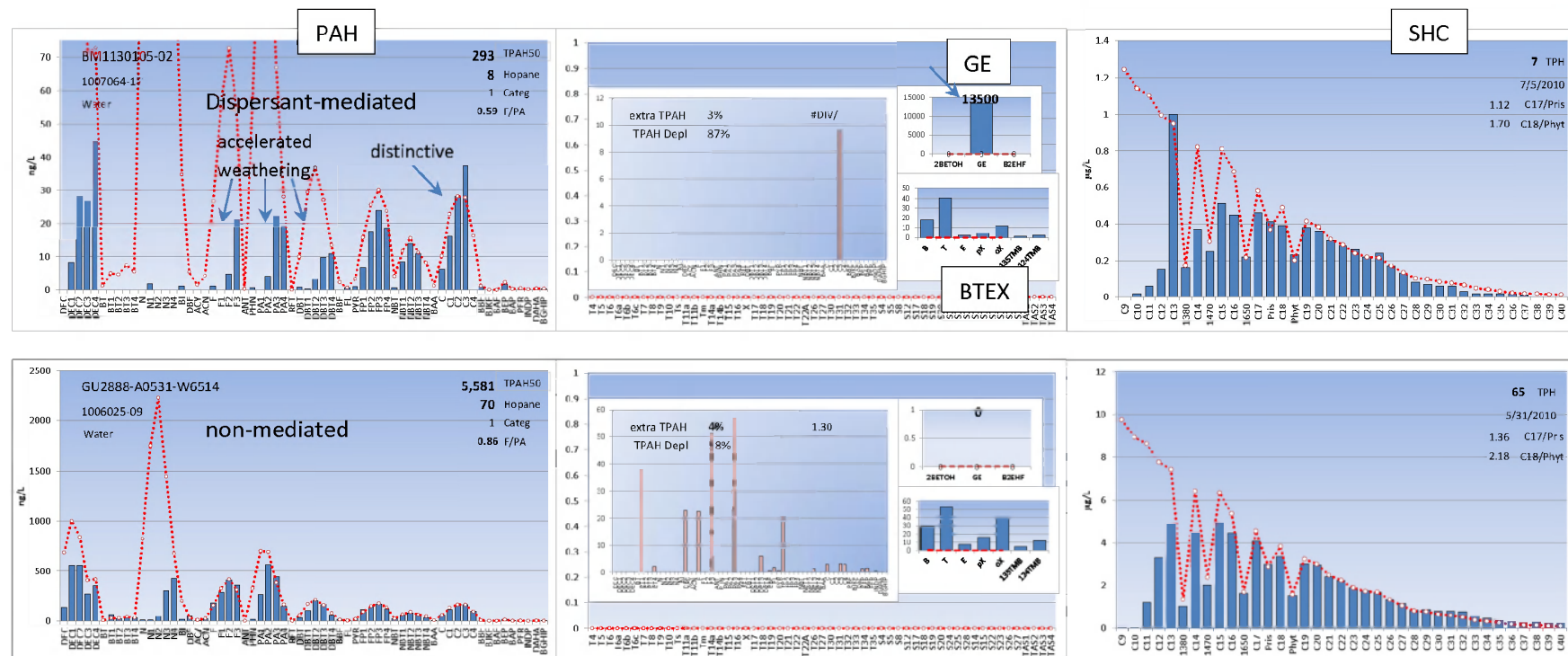
Figure 3. Dispersant effects on oil profiles. Typical deep-plume, dispersant-mediated, whole-water sample (top) shows heavily weathered PAH profile (left, overlaid with fresh MC252 reference–dotted red line scaled to C2-chrysene) with accelerated weathering of naphthalenes through C-3 dibenzothiophenes, the distinctive chrysenes (right PAH group), high levels of the glycol ethers (GE) dispersant indicator from Corexit 9500 (center upper-right plot), high concentrations of BTEX volatiles (center lower right plot), and unexpectedly fresh, only partially biodegraded saturates (SHC) (right plot) for the extent of PAH weathering. Compare with normal, non-dispersant-mediated, weathered sample in lower plots. Hopane was measured but biomarkers were not acquired. Sample and lab identifiers and lab matrix in upper left. Analyte abbreviations listed in Appendix 1.

5
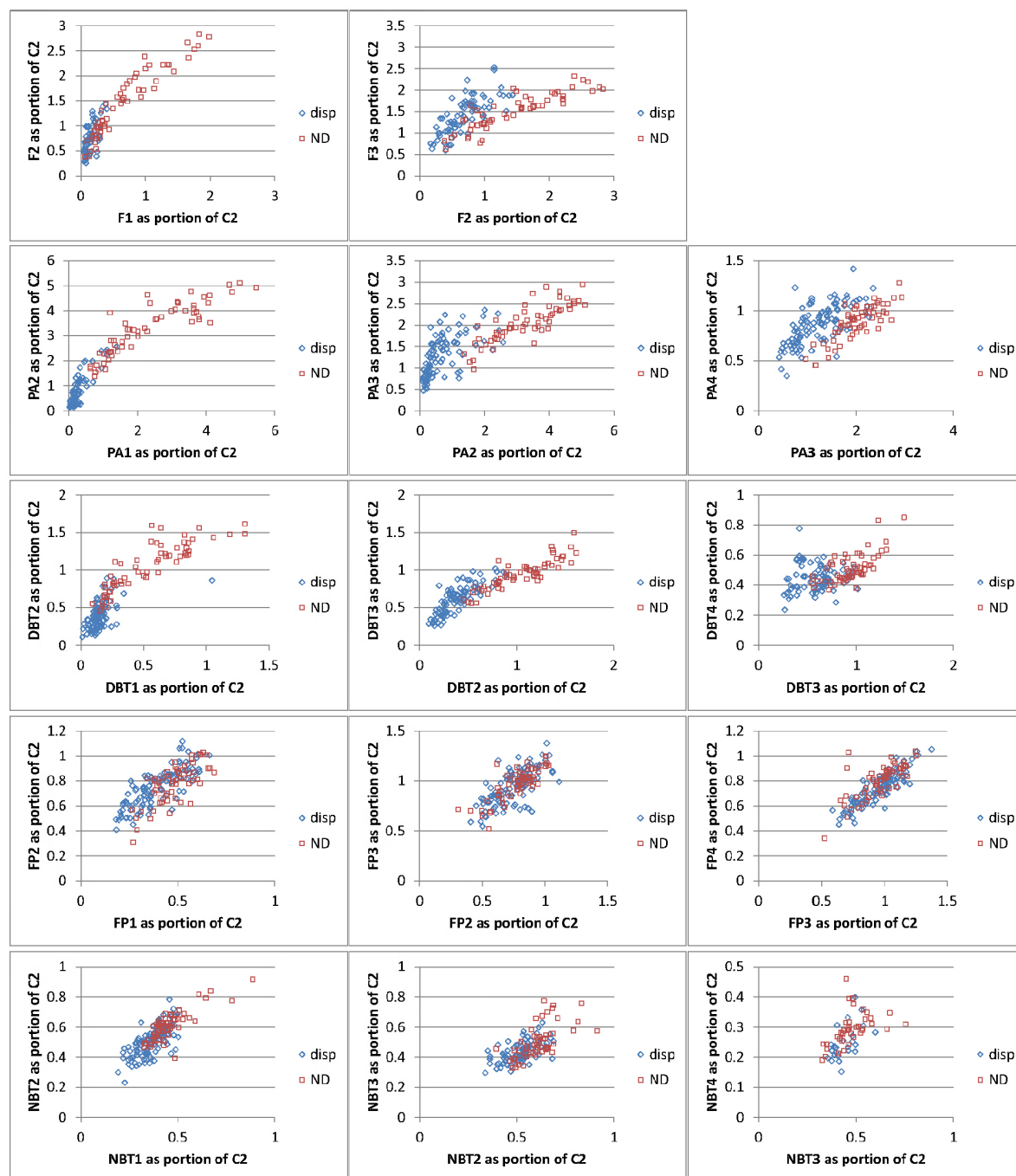
Figure 4. PAH distributions from dispersant-treated (blue) and untreated (red) water samples. All concentrations are "weather"normalized to the sample's C2-chrysene. Samples are MC252 matched particulate samples with no dissolved components; n = 110 dispersed, 58 non-dispersed. Pattern shifts towards left in dispersant-treated samples suggest more rapid analyte removal for the group (statistics in Table 1). The lower molecular weight and less alkylated PAHs (upper rows) showed the most rapid weathering and thus appeared clustered away from the non-dispersed group. The recalcitrant, higher alkylated NBTs show the least differences in weathering rates (bottom row).

6

Table 1. **Statistical significance of differences in treatments in Figure 4 using Mann-Whitney U test for bivariate data; one-tailed, alpha = 0.05. Only 3 digits of p-value are presented.**

parameter	p-value	significant	parameter	p-value	significant	parameter	p-value	significant
F1 vs F2	0.000	yes	F2 vs F3	0.000	yes	na		
PA1 vs PA2	0.000	yes	PA2 vs PA3	0.000	yes	PA3 vs PA4	0.000	yes
DBT1 vs DBT2	0.000	yes	DBT2 vs DBT3	0.000	yes	DBT3 vs DBT4	0.000	yes
FP1 vs FP2	0.001	yes	FP2 vs FP3	0.475	no	FP3 vs FP4	0.001	yes
NBT1 vs NBT2	0.094	no	NBT2 vs NBT3	0.314	no	NBT3 vs NBT4	0.290	no

Spier et al. (2013), also using DWH NRDA data, independently concluded that application of subsurface dispersants increased hydrocarbon concentrations at depth based on total hydrocarbon detects and concentrations but did not document any finer insights to the process. These results were further corroborated by controlled tank tests (Brandvik et al. 2013 and Johansen et al., 2013) demonstrating both the dispersant's effectiveness in breaking up the oil droplets, plus the hypothesized but heretofore undocumented, accelerated stripping of lower- and intermediate-molecular-weight PAH from the oil droplets and their transfer into the dissolved phase (NRC 2005). These analyses and other DWH field data confirmed that the dispersants injected at depth actually worked, i.e. they both reduced droplet size and accelerated dissolution of oil components.

Identifying Dispersant-mediated samples

Dispersant-mediated weathering effects were markedly different from normal oil-seawater dissolution patterns (Figure 3 and detailed below). Seven characteristics of the hydrocarbon profiles distinguished a dispersant-mediated sample:

1. Presence of dispersant (often at very high concentrations); DOSS, glycol ethers (GE), or 2-butoxyethanol (2BE). The 2BE was also a confounding contaminant in filtered samples. For unknown reasons, the third indicator, bis(2-ethylhexyl)fumerate, was not a reliable indicator. Note that some early samples were not analyzed for dispersants (begun at Alpha Laboratory on 25 July 2010).
2. A very weathered PAH profile with accelerated loss of light ends up through dibenzothiophenes.
3. A very distinctive water-washed chrysene pattern with C0<C1<C2<C3<C4.
4. Significant SHC often present, not completely microbially degraded based on n-C_{17}/pristane and n-C_{18}/phytane ratios.
5. Dibenzothiophene/phenanthrene (D/P) ratios on atypical low trend path in double-ratio plots (D2/P2 vs D3/P3).
6. Decalins, the dominant "pseudo-PAH" in Corexit, may be present and sometimes high, and
7. Dissolved samples usually contain excess fluorenes relative to phenanthrenes.

For fingerprinting purposes (Payne and Driskell 2015b), the uniquely weathered PAH patterns necessitated compiling a new dispersant-mediated reference series (Figure 5). Unexpectedly, in this series of dispersed particulate oil samples, there appeared markedly unweathered n-alkanes relative to the PAH weathering. Generally, SHC constituents are microbially degraded at a much higher rate than PAH, but these patterns suggested that the samples close to the wellhead had only undergone limited microbial

degradation. Seemingly, the PAH were being removed by abiotic dissolution processes—presumably having been stripped into the water-column from the extremely small, chemically-dispersed oil-phase threads and droplets (Figure 1and Figure 2) even before the microbial degradation of susceptible n-alkanes had begun. The partially degraded SHC profile in the first weathered sample (#2; Figure 5) is likely due to initial dissolution losses of the more soluble, shorter-chain ($<C_{13}$) n-alkanes compared to their higher-molecular-weight counterparts (McAuliffe 1987; Reddy et al. 2012; Payne and Beegle-Krause 2011).

As weathering advances, additional loss of n-alkanes is more attributable to biodegradation as reflected in the biodegradation index ratios, C_{17}/pristane and n-C_{18}/phytane whereby the straight-chained n-alkanes are degraded slightly faster than the branched alkanes, pristane and phytane (NRC 1985). Throughout most of the reference series (Figure 5), both the SHC and the biodegradation rates remain relatively constant until the final few stages. Compared to non-dispersed particulate oil samples (discussed below and in Payne and Driskell, 2015b), at every oil depletion stage in the series, the dispersed samples' indices show their PAH to be more degraded than the normally-weathered particulate samples (Figure 6).

Further afield, the SHC eventually disappeared. In the deepwater plume at distances greater than 32-64 km (Figure 7a-c), there was extensive microbial degradation as C_{17}/pristane and n-C_{18}/phytane ratios both decreased to zero values. In more coherent surface slicks, however, Stout (2015b) documented delayed changes in n-C_{17}/pristane and n-C_{18}/phytane ratios and losses of higher-molecular-weight waxes, relative to hopane, until the oil stranded in intertidal regimes. This was likely due to solar and emulsification processes creating an outer-skin barrier to weathering effects (Irvine et al. 1999, 2007; Ryan Rogers, personal communication, May 5, 2015).
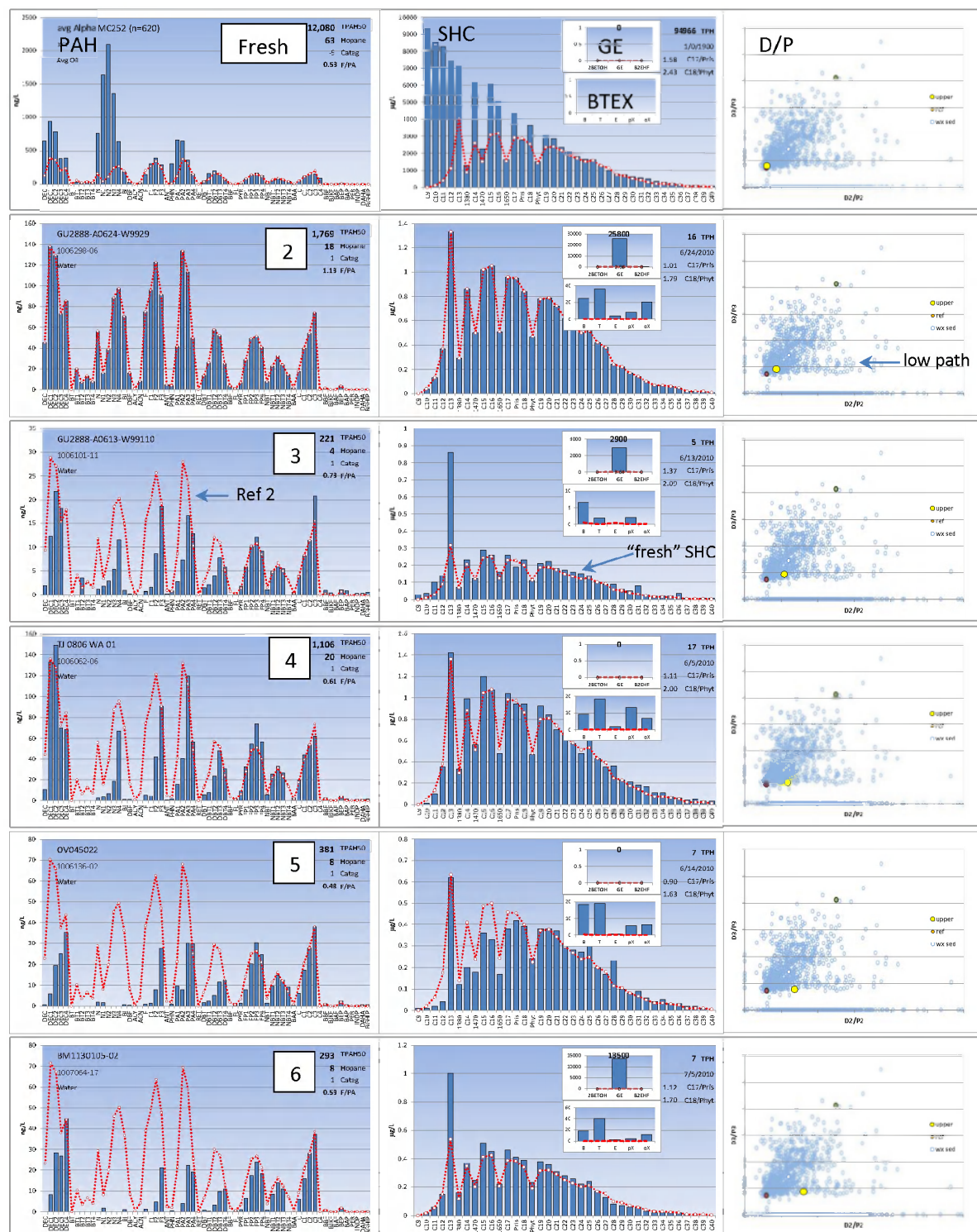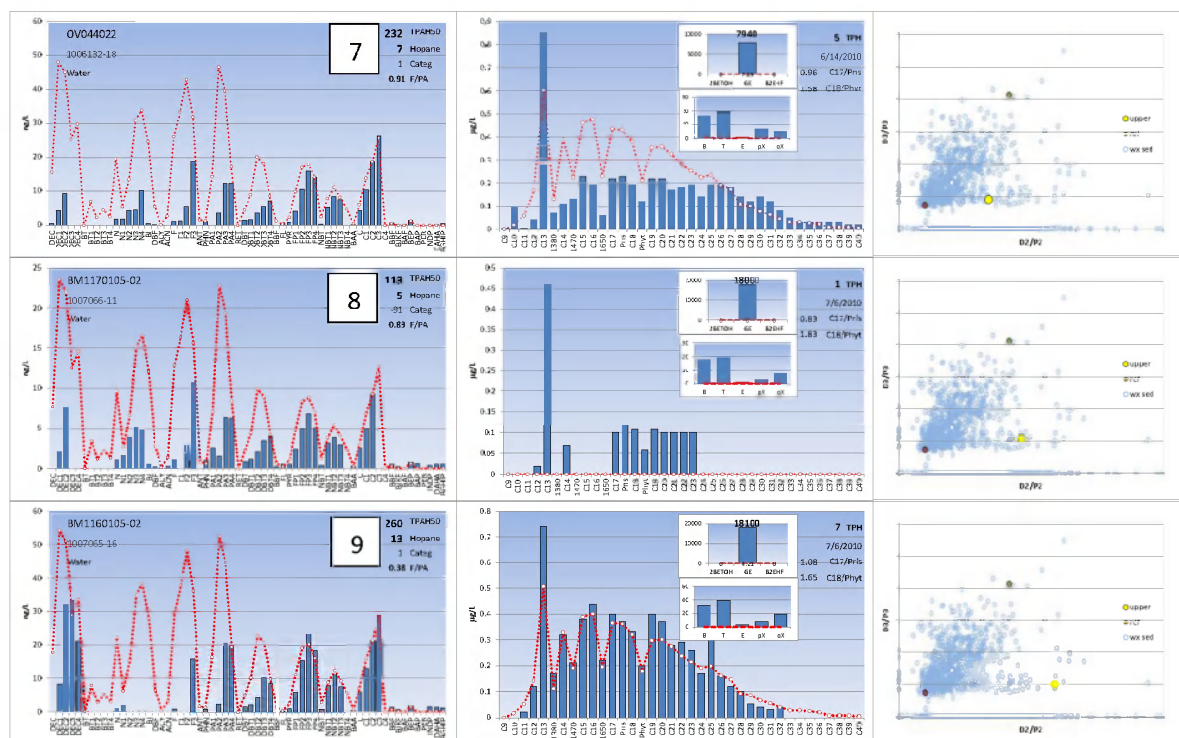
Figure 5. **Reference series of dispersant-mediated samples beginning with fresh oil (non-dispersed). Red line overlay is dispersed reference 2 scaled to NBT2 in PAH plots (left). Center plots of SHC are scaled to fresh n-C$_{26}$. Yellow dot in far-right D/P plots shows low path progression; dispersant glycol ethers (GE) and BTEX in center inset plots (red lines are method blanks). Samples without GE values were not analyzed for dispersants.**
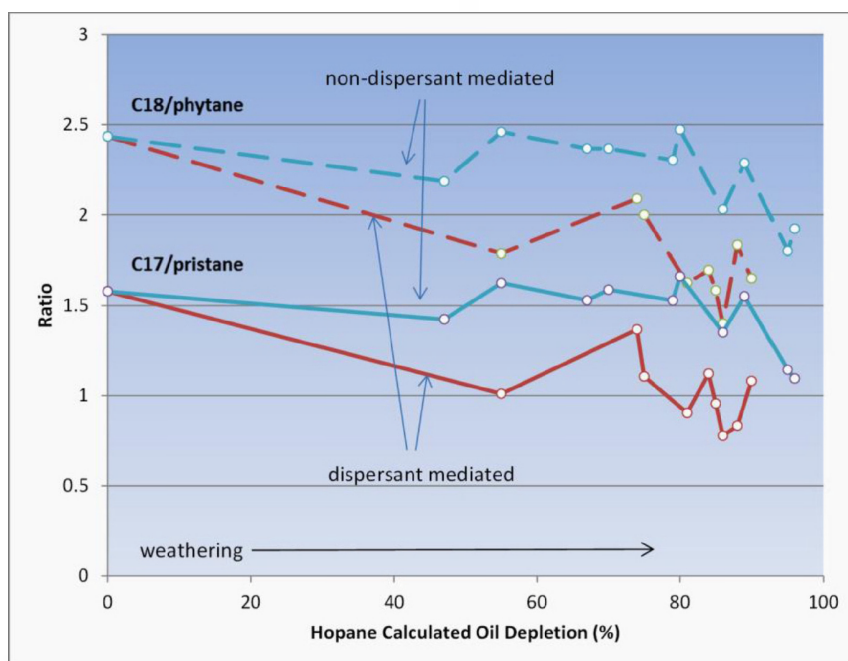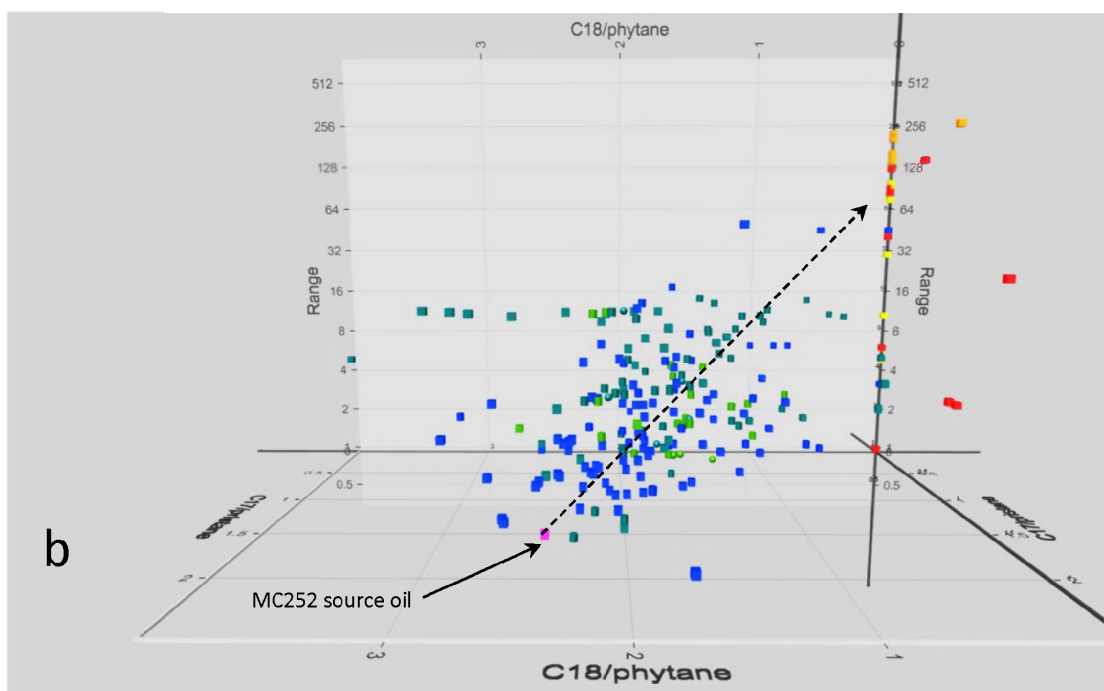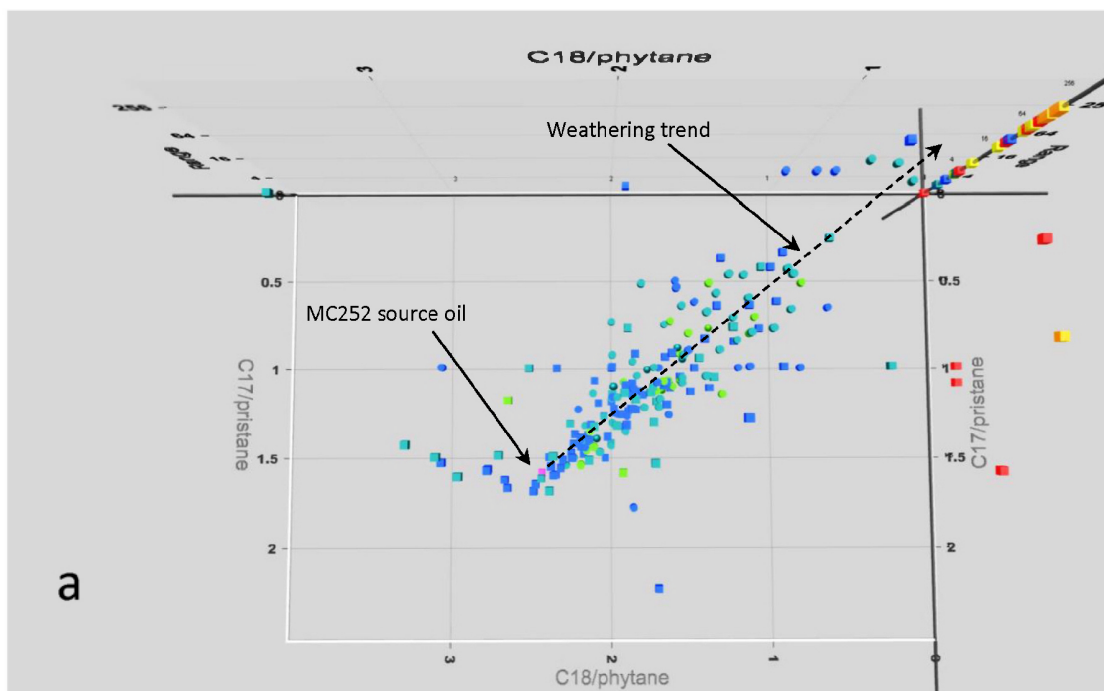

Figure 6. **Diagnostic SHC biodegradation ratios of non-dispersed and dispersed reference series samples (from Figure 5).**
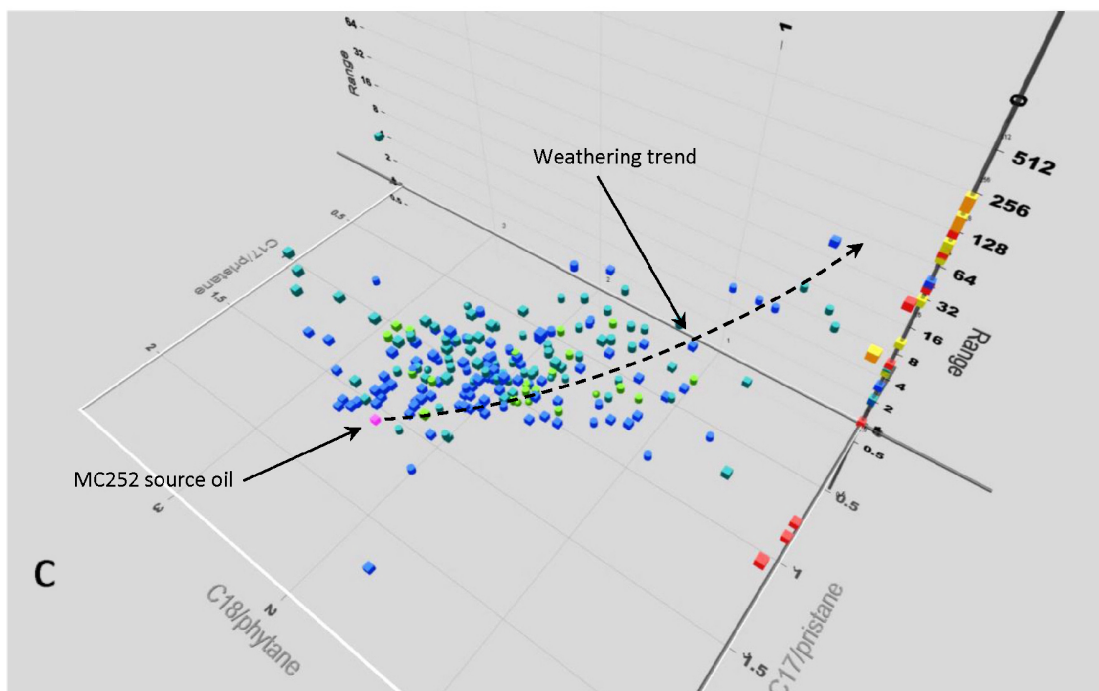
Figure 7a-c. Views of SHC diagnostic weathering ratios, C17/pristane and C18/phytane versus range (distance from wellhead) (km) and collection dates (colors). Blue, dark green and light green represent the initial May, June and July sampling periods. Other colors, samples with no C17 or C18 remaining, progress to December 2010. Spheres are dispersed samples, cubes are non-dispersed.

As a result of smaller droplets and more rapid dissolution, the dibenzothiophene/phenanthrene (D/P) ratios (Douglas et al. 1996) of dispersant-mediated samples trend along a distinctive "lower path" across the D/P double ratio plot (Figure 8a-c). This lower path behavior appears to be substantially driven by accelerated removal of C2-phenanthrenes and to a lesser extent, C2-dibenzothiophenes, while for unknown empirical reasons, the D3/P3 ratio remains more constant (Figure 8).

For these samples, the hopane-balance method used so effectively for assessing non-dispersed samples (Payne and Driskell 2015b, Forensic Fingerprinting Methods) was not as reliable. Typically, these highly weathered, dispersed samples were also low-TPAH-concentration samples with very low expected hopane. Rather than striving for a hopane-balance closure in the minor percent differences, for these low-hopane dispersant-mediated samples, the assessment was more about being in the right magnitude for expected hopane abundance.
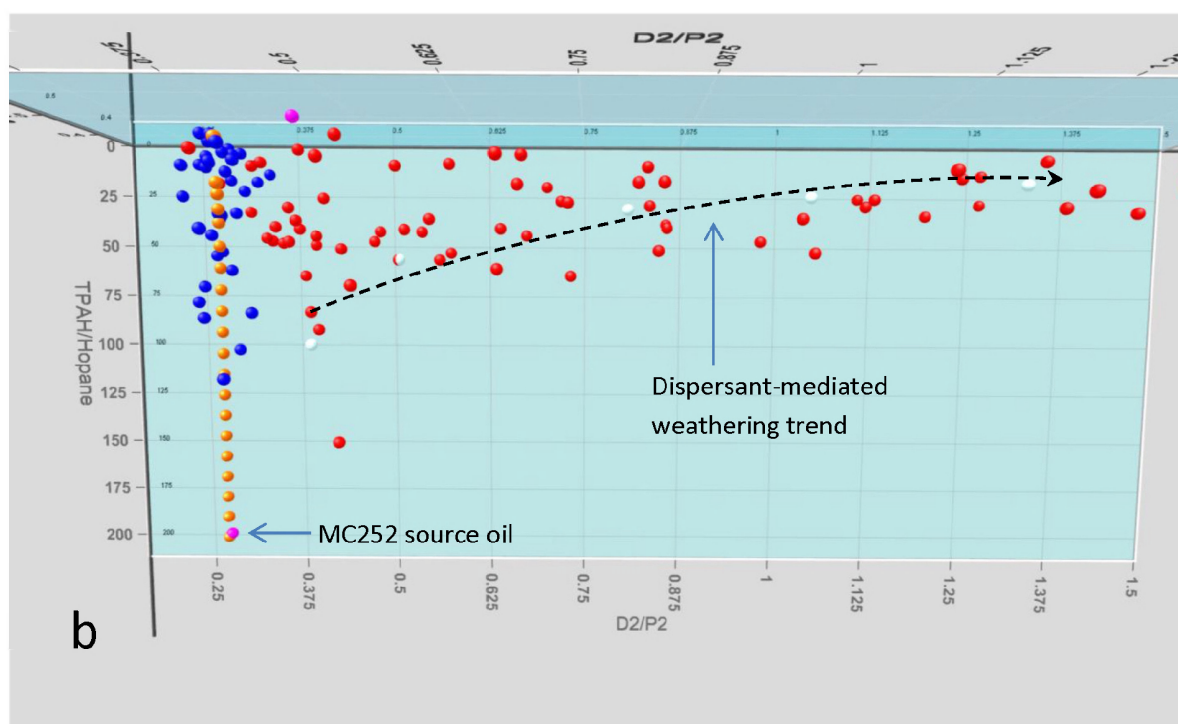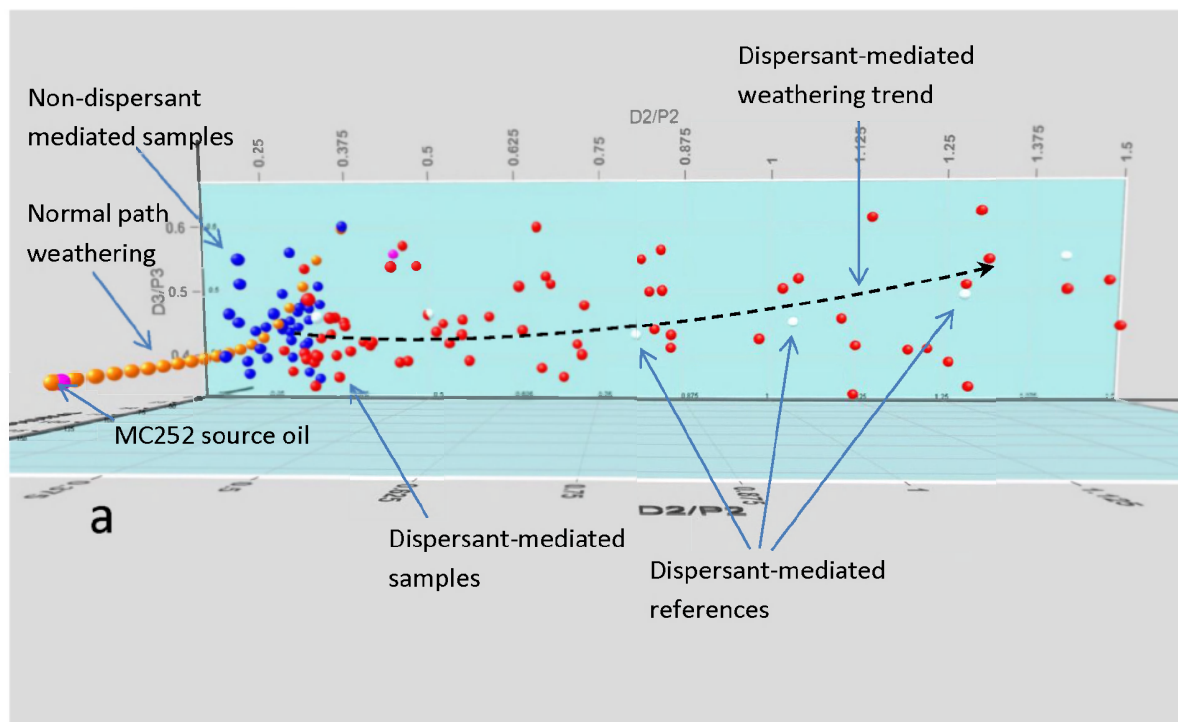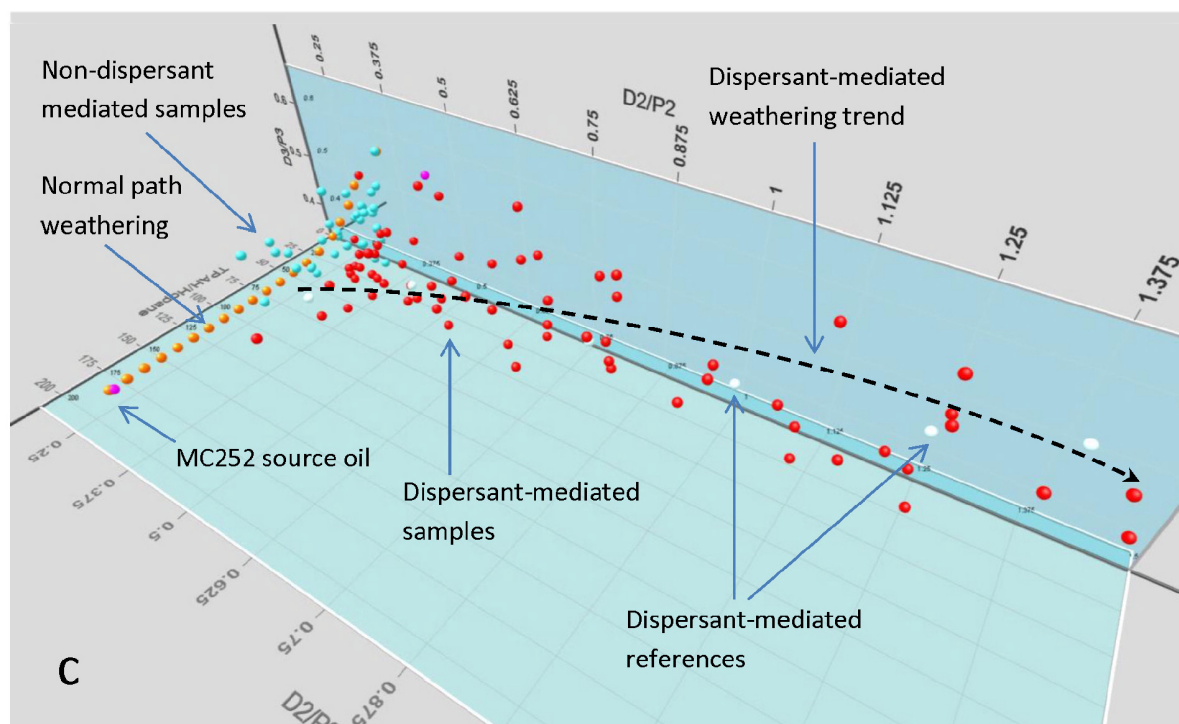
Figure 8a-c. TPAH/hopane, D2/P2 and D3/P3 for MC252-matched, particulate field samples from early cruises. Front, top and oblique views. Like "normal" weathered samples, dispersed samples quickly traverse the TPAH/hopane dimension (towards the back wall) from the source oil via rapid dissolution of lighter components but then sidetrack onto a completely novel path as the D/P ratios reflect the accelerated dissolution from smaller droplets.

Dispersant-mediated oil samples also exhibit accelerated losses of fluorenes that, as might be predicted from their dissolution constants (K_{ow} values), are removed even faster than phenanthrenes (Figure 4). Using the sum of fluorenes/sum of phenanthrenes as an index, dispersed samples typically show enhanced fluorene/phenanthrene ratios in dissolved phase (Figure 9) relative to source oil (0.53), and conversely, lower values in the fluorine-depleted particulate phase. This simplistic transfer model becomes more complex to evaluate in environmental samples when, for instance, a dispersant-mediated particulate sample picks up additional dissolved-phase components (Payne and Driskell, 2015b). Dispersant-treated ("chemically enhanced") water-accommodated-fractions (CEWAF extracts) generated for Trustee toxicity studies were also noted to contain enhanced dissolved-fluorene concentrations. It is not known if the elevated dissolved-phase fluorene increases toxicity in the field but they, and possibly other PAH, are certainly more bioavailable to enhance exposure after dispersant treatment. Incardona et al. (2004, 2005, 2014) and Brette (2014) noted that exposure to weathered crude oil or individual tricyclic PAHs (fluorene, dibenzothiophene and phenanthrene) in laboratory studies caused specific defects in cardiac rate, rhythm, and contractility in zebrafish embryos soon after the heart became functional.

As listed above, the presence of both unexpectedly fresh SHC and decalins also correlated with dispersant use. While the delayed SHC degradation seemed purely a dispersant effect, decalins, unfortunately, occurred in both MC252 and the Corexit blends and thus, confounded interpretation. Mostly, they simply alerted us to the possibility of dispersant effects.

14
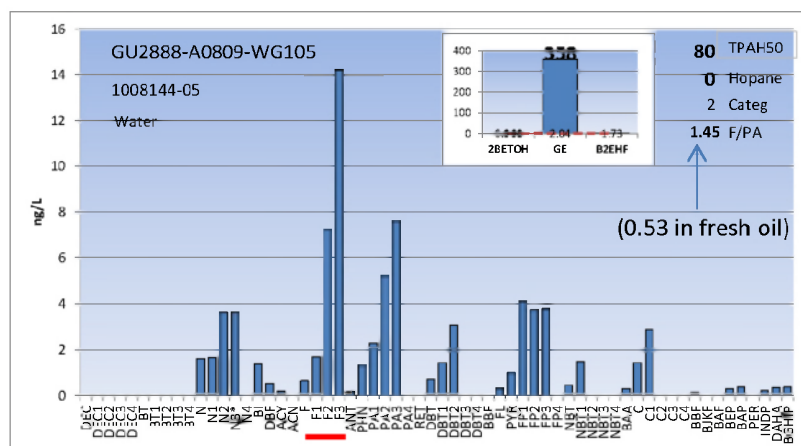
Figure 9. Example of enhanced fluorenes in dispersant-mediated, dissolved-phase sample. Sum of fluorenes to sum of phenanthrenes was 1.45 (relative to 0.53 in fresh oil) that suggests that particulate oil passing through this water parcel was exposed to dispersant (GE in inset plot) and had lost fluorenes faster than phenanthrenes that were then incorporated into this sample. The effect is also implied in upper rows of Figure 4 comparing the accelerated shifts of fluorenes relative to the phenanthrene homologues.

Microbial SHC Degradation

Oil biodegradation is a complex process involving both microbial communities in the water-phases as well as microbes attaching to oil surfaces (Brakstadt et al., 2015). Conceptually, dissolved hydrocarbons are more readily available for microbes in that they would not need to be extracted from a solid matrix but conversely, they would be diffused in a water parcel and thus, could also be a less concentrated resource. With particulate phase oil, microbes work the surface of oil droplets by first exuding extracellular substances to attach themselves to the substrate and then release the extracellular enzymes (mostly mono- and dioxygenases in aerobic circumstances) to break down and selectively capture and transport otherwise insoluble hydrocarbons back across the cellular membrane (Gutierrez et al. 2013). Breaking the oil into smaller droplets would increase the oil-water interface, the space available for microbial attachment and growth. Not surprisingly, several laboratory studies have shown that dispersants can increase biodegradation (Siron et al., 1995; Venosa and Holder 2007; Prince et al. 2013; McFarlin et al. 2014; Brakstad et al., 2014). Brakstad et al. (2015) further demonstrate that biodegradation correlates with droplet sizes in dispersion; faster biotransformation of the low-range and medium-range MW n-alkanes was measured in the 10 μm than the 30 μm dispersions; they conclude that the use of dispersants to generate small droplets will promote biodegradation in seawater under otherwise similar environmental conditions.

However, the lack of significant microbial aliphatic degradation in high dispersant-mediated, DWH samples close to the wellhead does not support this enhancement concept (Figure 7). This may be due to an inhibitory effect from the C_5-C_{10} homologues (e.g., pentane, hexane, heptane, octane, nonane, and decane) (Bartha and Atlas 1977) and the mono-cycloaliphatic compounds (e.g., cyclopentane, cyclohexane, and cycloheptane) (Leahy and Colwell, 1990) that were in high concentrations close to the wellhead early in the spill (Payne and Driskell, 2015a). Acting as solvents, they tend to disrupt lipid membrane structures of microorganisms. Other studies have noted that highly concentrated dispersed oil droplets, BTEX, or surfactants may initially inhibit microbial degradation of hydrocarbons until PAH and SHC are diluted to levels more suitable to their metabolic or extracellular exudates' functionality (Prince

15

et al. 2013). Likewise, initial microbial degradation at depth may have been carbon rich but nutrient limited (Edwards, et al., 2011). Campo et al. (2013), Brakstad et al. (2015) and Venosa (EPA, personal communication, 22 Jan 2013) also noted inhibited or delayed n-alkane degradation in oil/dispersant/microcosm studies at $5°$ C and from these studies concluded that the inhibition may have been due to the impermeability of a suggested waxy, solid-phase state of the SHC fraction at that temperature. These findings are in direct contrast to Hazen et al. (2010) concluding from a smaller, early DWH data set that most, if not all, aliphatics were microbially degraded within a few weeks (half-lives of 1.2-6.1 days). These interpretations were also discussed by Valentine et al. (2010, 2011) who concluded that currents, mixing processes, and autoinoculation would affect priming of native microbiota and subsequent bioremediation processes. Despite these contrasting findings, clearly, with additional time and distance from the wellhead, aliphatic microbial degradation of both dispersant- and non-dispersant-treated oil was comprehensive in zeroing out their n-C_{17}/pristane and n-C_{18}/phytane ratios (Figure 7). Away from the wellhead, microbial succession and hydrocarbon-degrading abilities are well documented (reviewed by Kimes et al. 2014).

Summary and Implications

Dispersant indicators, measured for the first time in field-collected, particulate-phase oil samples at depth, document the utility of dispersant injections at the wellhead for reducing oil-droplet sizes and thus, limiting oil rising to the surface and potentially being transported to shorelines. Dispersant application at depth also resulted in markedly enhanced dissolution of lower- and intermediate-molecular-weight PAH compared to non-dispersant-treated oil. Once dissolved, these components move with the plume (not buoyantly rising in the water column like larger oil droplets) but are still subject to microbial degradation. Enhanced dissolution and retention at depth also suggests increased bioavailability of BTEX and PAH to benthic and pelagic organisms.

Elucidating the effects of dispersants on oil droplets at depth was a fortunate finding. Without the opportune convergence of a clean ocean background, an entrained plume, and high dispersant and oil concentrations, dispersant-mediated profiles would have been difficult to isolate. Relying solely on the PAH data, these samples would have been enigmatically classified as a mixture or "other oil." Furthermore, the now revealed physical/chemical dynamics of accelerated PAH depletion (up through dibenzothiophenes) will certainly instigate further investigations into dispersant/oil interactions. Samples with actual dispersant-modified profiles (i.e., not just containing dispersant indicators) comprised 318 of the 1,768 MC-252-matched water samples with the furthest in the plume, 183 km southwest of the wellhead. Dispersant indicators were found out to 412 km from the wellhead. A year later, in 2011, dispersant indicators were still detected in deep-bottom flocculants, thus corroborating a "dirty blizzard" scenario (Passow et al., 2012; Schrope 2013).

References

Aprin, L., F. Heymes, P. Lauret, P. Slangen, S. Le Floch. (2015). Experimental characterization of dispersant addition on rising oil droplets in water column. *Chemical Engineering Transactions* 43: 2287-2292 DOI: 10.3303/CET1543382

Bartha, R. and R.M. Atlas. 1977. The microbiology of aquatic oil spills. In: D. Perlman (ed.), <u>Advances in Applied Microbiology</u>. Academic Press, pp. 225-266.

16

Bejarano A.C., E. Levine, A.J. Mearns. (2013). Effectiveness and potential ecological effects of offshore surface dispersant use during the Deepwater Horizon oil spill: a retrospective analysis of monitoring data. *Environmental Monitoring and Assessment* 185(12), 10281-10295. http://dx.doi.org/10.1007/s10661-013-3332-y.

Brakstad, O.G., P.S. Daling, L.-G. Faksness, I.K. Almas, S.-H.Vang, S. Syslak, F. Leirvik. (2014). Depletion and biodegradation of the Macondo 252 oil in dispersions and emulsions generated in an oil-on-seawater mesocosm flume basin. *Mar. Poll. Bull.* 84, 125-134.

Brakstad, O. G., T. Nordtug, M. Throne-Holst. (2015). Biodegradation of dispersed Macondo oil in seawater at low temperature and different oil droplet sizes. *Mar. Poll. Bull.* 93: 144–152

Brandvik, P.J., Ø. Johansen, F. Leirvik, U. Farooq, P.S. Daling. (2013). Droplet breakup in subsurface oil releases – Part 1: Experimental study of droplet breakup and effectiveness of dispersant injection. *Marine Pollution Bulletin* 73(1): 319-326.

Brette, F., B. Machado, C. Cros, J.P. Incardona, N.L. Scholz, B.A. Block. (2014). Crude Oil Impairs Cardiac Excitation-Contraction Coupling in Fish. *Science* 343:6172, 772-776, DOI: 10.1126/science.1242747

Campo, P., A.D. Venosa, and M.T. Suidan (2013). Biodegradability of Corexit 9500 and dispersed South Louisiana crude oil at 5 and 25° C. *Environ. Sci. Technol.* 47: 1960-1967.

Driskell, W.B., and J.R. Payne. (2015). Forensic Assessment of 2010 DWH Nearshore Water Samples. PECI Technical Report to the Trustees in support of the PDARP.

Douglas, G.S., A.E. Bence, R.C. Prince, S.J. McMillen, and E.L. Butler. (1996). Environmental stability of selected petroleum hydrocarbon source and weathering ratios. *Environ, Sci. Technol.* 30(7): 2332-2339.

Edwards, B.R., C.M. Reddy, R. Camilli, C.A. Carmichael, K. Longnecker, and B.A.S. Van Mooy. (2011). Rapid microbial respiration of oil from the Deepwater Horizon spill in offshore surface waters of the Gulf of Mexico. *Environ. Res. Lett.* 6: 035301.

Gopalan B. and J. Katz (2010). Turbulent shearing of crude oil mixed with dispersants generates long microthreads and microdroplets. *PRL* 104, 054501, 4 pp.

Gray, J.L., L.K. Kanagy, E.T. Furlong, J.W. McCoy, and C.J. Kanagy. (2011). Determination of the anionic surfactant di(ethylhexyl)sodium sulfosuccinate in water samples collected from Gulf of Mexico coastal waters before and after landfall of oil from the Deepwater Horizon oil spill, May to October, 2010. U.S. Geological Survey Open-File Report 2010-1318, 15 p <http://www.pubs.usgs.gov/of/2010/1318/>

Gray, J.L., L.K. Kanagy, E.T. Furlong, C.J. Kanagy, J.W. McCoy, A. Mason, and G. Lauenstein. (2014). Presence of the Corexit component dioctyl sodium sulfosuccinate in Gulf of Mexico waters after the 2010 Deepwater Horizon oil spill. *Chemosphere* 95: 124-130.

Gutierrez, T., D. Berry, T. Yang, S. Mishamandani, L. McCKay, A. Teske, and M.D. Aitken. (2013). Role of bacterial exopolysaccharides (EPS) in the fate of the oil released during the Deepwater Horizon

17

oil spill. *PLOS ONE* 8(6): e67717

Hazen T.C., E.A. Dubinsky, T.Z. DeSantis *et al.* (2010) Deep-sea oil plume enriches indigenous oil-degrading bacteria. *Science* 330: 204-208.

Incardona, J.P., T.K. Collier, N.L. Scholz. (2004). Defects in cardiac function precede morphological abnormalities in fish embryos exposed to polycyclic aromatic hydrocarbons. *Toxicol. Appl. Pharmacol.* 196, 191-205.

Incardona, J.P., M.G. Carls, H. Teraoka, C.A. Sloan, T.K. Collier, N.L. Scholz. (2005). Aryl hydrocarbon receptor-independent toxicity of weathered crude oil during fish development. *Environ. Health Perspect.* 113, 1755-1762.

Incardona, J.P., L.D. Gardner, T.L. Linbo, T.L. Brown, A.J. Esbaugh, E.M. Mager, J.D. Stieglitz, B.L. French, J.S. Labenia, C.A. Laetz, M.Tagal, C.A. Sloan, A. Elizur, D.D. Benetti, M. Grosell, B.A. Block, and N.L. Scholz. (2014). Deepwater Horizon crude oil impacts the developing hearts of large predatory pelagic fish. *PNAS* 111 (15) E1510-E1518; doi:10.1073/pnas.1320950111

Irvine, G. V., D. H. Mann, and J. W. Short. (1999). Multi-year persistence of oil mousse on high energy beaches distant from the *Exxon Valdez* spill origin. *Mar. Poll. Bull.* 38(7):572-584.

Irvine, G. V., D. H. Mann, and J. W. Short. (2007). Monitoring lingering oil from the *Exxon Valdez* spill on Gulf of Alaska armored beaches and mussel beds sixteen years post-spill. *Exxon Valdez* Oil Spill Restoration Project Final Report, (Restoration Project 40708), U.S. Geological Survey, Alaska Science Center, Anchorage, Alaska, 81 p.

Johansen, Ø, P.J. Brandvik, U. Farooq. (2013). Droplet breakup in subsea oil releases – Part 2: Predictions of droplet size distributions with and without injection of chemical dispersants. *Mar. Poll. Bull.*, 73(1): 327-335.

Katz, J. (2009). Measurements and modeling of size distributions, settling, and dispersions (turbulent diffusion) rates. Final Report prepared for the Coastal Response Research Center. August 2009. 31 pp.

Kimes, N. E., A.V. Callaghan, J.M. Suflita and P.J.Morris. (2014). Microbial transformation of the Deepwater Horizon oil spill—past, present, and future perspectives. *Front. Microbiol.* 5:603. doi:10.3389/fmicb.2014.00603

Kujawinski, E.B., M.C.K. Soule, D.L. Valentine, A.K. Boysen, K. Longnecker, and M.C. Redmond. (2011). Fate of dispersants associated with the Deepwater Horizon oil spill. *Environ. Sci. Technol.* 45(5): 1298-1306.

Leahy, J.G. and R.R. Colwell. (1990). Microbial degradation of hydrocarbons in the environment. *Microbiological Reviews* 54(3), 305-315.

McAuliffe, C.D. (1987). Organism exposure to volatile/soluble hydrocarbons from crude oil spills – a field and laboratory comparison. *Proceedings of the 1987 International Oil Spill Conference*, American Petroleum Institute, Washington, D.C., pp. 275-288.

McFarlin, K.M., Prince, R.C., Perkins, R., Leigh, M.B., 2014. Biodegradation of dispersed oil in Arctic seawater at - 1_C. *PLOS ONE* 9, e84297.

Murphy DW, Li C, d'Albignac V, Morra D, Katz J. 2015. Splash behavior and oily marine aerosol production by raindrops impacting oil slicks. J. Fluid Mech. In Press.

National Research Council (NRC). (1985). Oil in the Sea: Inputs, Rates, and Effects. National Academy Press, Washington, D.C.

National Research Council (NRC). (2005). Oil Spill Dispersants: Efficacy and Effects. National Academy Press, Washington D.C., 377 pp.

Passow, U., K. Ziervogel, V. Asper, and A. Diercks. (2012). Marine snow formation in the aftermath of the Deepwater Horizon oil spill in the Gulf of Mexico. *Environ. Res. Lett.* 7. 11 pp.

Payne, J.R. and C.J. Beegle-Krause. (2011). Physical transport and chemical behavior of dispersed oil. Twenty-six page White Paper commissioned for the CRRC Workshop: The Future of Dispersant Use in Spill Response. September 20-22, 2011. NOAA Disaster Response Center, Mobile, Alabama. Available at: http://www.crrc.unh.edu/workshops/dispersant_future_11/Dispersant_Initiative_FINALREPORT.pdf).

Payne, J.R. and W.B. Driskell. (2015a). 2010 DWH offshore water column samples—Forensic assessments and oil exposures. PECI Technical Report to the Trustees in support of the PDARP.

Payne, J.R. and W.B. Driskell. (2015b). Forensic fingerprinting methods and classification of DWH offshore water samples. PECI Technical Report to the Trustees in support of the PDARP.

Payne, J.R. and W.B. Driskell. (2015c). Offshore adaptive sampling strategies. PECI Technical Report to the Trustees in support of the PDARP.

Prince, R.C., K.M. McFarlin, J.D. Butler, E.J. Febbo, F.C.Y. Wang, T.J. Nedwed, (2013). The primary biodegradation of dispersed crude oil in the sea, *Chemosphere*, 90(2): 521-526.

Reddy, C.M., J.S. Arey, J.S. Seewald, S.P. Sylva, K.L. Lemkau, R.K. Nelson, C.A. Carmichael, C.P. McIntyre, J. Fenwick, G.T. Ventura, B.A.S. Van Mooy, and R. Camilli. (2012). Composition and fate of gas and oil released to the water column during the Deepwater Horizon oil spill. *PNAS* 109 (50) 20229-20234.

Ryerson, T.B., T.B. Ryerson, K.C. Aikin,W.M. Angevine,E.L. Atlas, D.R. Blake, C.A. Brock, F.C. Fehsenfeld,R-S. Gao, J.A. de Gouw, D.W. Fahey, J.S. Holloway, D.A. Lack, R.A. Lueb, S. Meinardi, A.M. Middlebrook, D.M. Murphy, J.A. Neuman, J.B. Nowak, D.D. Parrish, J. Peischl, A.E. Perring, I.B. Pollack, A.R. Ravishankara, J.M. Roberts, J.P. Schwarz, J.R. Spackman, H. Stark, C. Warneke, and L.A. Watts. (2011). Atmospheric emissions from the Deepwater Horizon spill constrain air-water partitioning, hydrocarbon fate, and leak rate, *Geophys. Res. Lett.*, 38, L07803, doi:10.1029/2011GL046726.

Schrope, M. (2013). Dirty blizzard buried Deepwater Horizon oil. Nature News (Nature Publishing Group). On-line publication Jan 26, 2013.

19

Siron, R., Pelletier, E., Brochu, C., 1995. Environmental factors influencing the biodegradation of petroleum hydrocarbons in cold seawater. *Arch. Environ. Contam. Toxicol.* 28, 406-416

Spier, C., W.T. Stringfellow, T.C. Hazen, M. Conrad. (2013). Distribution of hydrocarbons released during the 2010 MC252 oil spill in deep offshore waters. *Env. Poll.* 173: 224-230.

Stout, S.A. (2015a). Review of dispersants used in response to the Deepwater Horizon oil spill. NewFields Technical Report to the Trustees in support of the PDARP.

Stout, S.A. (2015b). Range in composition and weathering among floating Macondo oils during the Deepwater Horizon oil spill. NewFields Technical Report to the Trustees in support of the PDARP.

Tabesh, H., S Ayatollahi, and M. Towhidi (2010) A simple powerful bivariate test for two sample location problems in experimental and observational studies. *Theor Biol Med Model.* 2010: 7:13; doi: 10.1186/1742-4682-7-13

Valentine, D.L., J.D. Kessler, M.C. Redmond, S.D. Mendes, M.B. Heintz, C.Farwell, L,Hu, F.S. Kinnaman, S.Yvon-Lewis, M.Du, E.W. Chan, F.Garcia Tigreros, C.J. Villanueva. (2010). Propane respiration jump-starts microbial response to a deep oil spill. *Science* 330:208-211.

Valentine, D.L., I. Mezic, S. Macesic, N. Crnjarc-Zic, S. Ivic, P.J. Hogan, V.A. Fonoberov, and S. Loire. (2011). Dynamic autoinoculation and the microbial ecology of a deepwater hydrocarbon irruption. *PNAS* 1 108820 109.

Venosa, A. (2013). Biodegradation of DOSS and Dispersed South Louisiana Crude oil at two temperatures. Presented at the Gulf of Mexico Oil Spill & Ecosystem Science Conference. January 21-23, 2013. New Orleans, LA.

Venosa, A.D., Holder, E.L., 2007. Biodegradability of dispersed crude oil at two different temperatures. *Mar. Poll. Bull.* 54, 545-553.

White, H.K., S.L. Lyons, S.J. Harrison, D.M. Findley, Y. Liu, and E.B. Kujawinski. (2014). Long-term persistence of dispersants following the Deepwater Horizon oil spill. *Environ. Sci. Technol. Lett.* 1: 295-299.

20

Appendix 1 – Hydrocarbon names and abbreviations used in report.

Polycylic Aromatic Hydrocarbons (PAH) with extended alkylated homologues

Abbrev	Compound		Abbrev	Compound		Abbrev	Compound
D0	cis/trans-Decalin		A0	Anthracene		BA0	Benz[a]anthracene
D1	C1-Decalins		P0	Phenanthrene		C0	Chrysene/Triphenylene
D2	C2-Decalins		PA1	C1-Phenanthrenes/Anthracenes		BC1	C1-Chrysenes
D3	C3-Decalins		PA2	C2-Phenanthrenes/Anthracenes		BC2	C2-Chrysenes
D4	C4-Decalins		PA3	C3-Phenanthrenes/Anthracenes		BC3	C3-Chrysenes
BT0	Benzothiophene		PA4	C4-Phenanthrenes/Anthracenes		BC4	C4-Chrysenes
BT1	C1-Benzo(b)thiophenes		RET	Retene		BBF	Benzo[b]fluoranthene
BT2	C2-Benzo(b)thiophenes		DBT0	Dibenzothiophene		BKF	Benzo[,k]fluoranthene
BT3	C3-Benzo(b)thiophenes		DBT1	C1-Dibenzothiophenes		BAF	Benzo[a]fluoranthene
BT4	C4-Benzo(b)thiophenes		DBT2	C2-Dibenzothiophenes		BEP	Benzo[e]pyrene
N0	Naphthalene		DBT3	C3-Dibenzothiophenes		BAP	Benzo[a]pyrene
N1	C1-Naphthalenes		DBT4	C4-Dibenzothiophenes		PER	Perylene
N2	C2-Naphthalenes		BF	Benzo(b)fluorene		IND	Indeno[1,2,3-cd]pyrene
N3	C3-Naphthalenes		FL0	Fluoranthene		DA	Dibenz[a,h]anthracene
N4	C4-Naphthalenes		PY0	Pyrene		GHI	Benzo[g,h,i]perylene
B	Biphenyl		FP1	C1-Fluoranthenes/Pyrenes			
DF	Dibenzofuran		FP2	C2-Fluoranthenes/Pyrenes			
AY	Acenaphthylene		FP3	C3-Fluoranthenes/Pyrenes			
AE	Acenaphthene		FP4	C4-Fluoranthenes/Pyrenes			
F0	Fluorene		NBT0	Naphthobenzothiophenes			
F1	C1-Fluorenes		NBT1	C1-Naphthobenzothiophenes			
F2	C2-Fluorenes		NBT2	C2-Naphthobenzothiophenes			
F3	C3-Fluorenes		NBT3	C3-Naphthobenzothiophenes			
			NBT4	C4-Naphthobenzothiophenes			

Saturated Hydrocarbons (n-alkanes and isoprenoids)

Abbr.	Analyte		Abbr.	Analyte
C9	n-Nonane		C23	n-Tricosane
C10	n-Decane		C24	n-Tetracosane

21

C11	n-Undecane	C25	n-Pentacosane
C12	n-Dodecane	C26	n-Hexacosane
C13	n-Tridecane	C27	n-Heptacosane
1380	2,6,10 Trimethyldodecane	C28	n-Octacosane
C14	n-Tetradecane	C29	n-Nonacosane
1470	2,6,10 Trimethyltridecane	C30	n-Triacontane
C15	n-Pentadecane	C31	n-Hentriacontane
C16	n-Hexadecane	C32	n-Dotriacontane
nPr	Norpristane	C33	n-Tritriacontane
C17	n-Heptadecane	C34	n-Tetratriacontane
Pr	Pristane	C35	n-Pentatriacontane
C18	n-Octadecane	C36	n-Hexatriacontane
Ph	Phytane	C37	n-Heptatriacontane
C19	n-Nonadecane	C38	n-Octatriacontane
C20	n-Eicosane	C39	n-Nonatriacontane
C21	n-Heneicosane	C40	n-Tetracontane
C22	n-Docosane		

Volatiles (BTEX)

Abbrev	Analyte
B	Benzene
T	Toluene
E	Ethylbenzene
X	total-Xylenes

22